Transonic Thermal Blooming due to an Intense Laser Beam

E. Fenton Carey* and Allen E. Fuhs†
Naval Postgraduate School, Monterey, Calif.

According to the linearized solutions for thermal blooming, the density perturbations become infinite (i.e., "castastrophic" defocusing) as the Mach number approaches unity. However, the nonlinearities in the transonic equations terminate the trend to infinity. The nonlinear equations, which are formulated in natural coordinates, with heat addition are transformed into simple linear algebraic equations through the specification of the streamline geometry in the heat release region. At a Mach number of unity, streamtube area variation was found to be directly proportional to the change in total temperature. A steady, two-dimensional, mixed flow solution has been obtained for the transonic thermal blooming problem. The solution for the density perturbations within a laser beam at a Mach number of precisely unity is given. For a Gaussian beam with an intensity of 3.333×10^{7} W/m^2 and an atmospheric absorption of 8.0×10^{-7}cm^{-1}the maximum fractional density perturbation is 1.028×10^{-4}. The transonic thermal blooming problem does not pose as serious a problem as previously anticipated.

Nomenclature

A = area, square centimeters
a = speed of sound, m/sec
b = function, dimensionless
c = speed of light, m/sec
C_p = specific heat at constant pressure, J/kg mass ($^\circ K$)
G = function specified by Eq. (12), dimensionless
h = specific enthalpy, J/kg mass
I = laser beam intensity, W/cm^2; also integral function representation
k = Gladstone-Dale constant, m^3/kg mass
L = length, m; also, functional representation of normalized velocity, dimensionless
M = Mach number, dimensionless
N = number of waves, dimensionless
n = normal coordinate, centimeters; also index of refraction, dimensionless
p = static pressure, N/m^2
Q = heat source, W/cm^3
R = universal gas constant, J/kg mass ($^\circ K$); also radius of curvature, cm
r = distance, cm
r^* = distance from laser output aperture to position in beam having preceisely Mach 1.0 flow
s = streamline coordinate, cm
T = static temperature, °K
t = maximum streamtube thickness, cm
U,u = speed (x-direction), m/sec
w = laser beam spot size, cm
x = coordinate, cm
y = coordinate, cm
Z = streamtube shape, cm
α = atmospheric absorption, cm^{-1}
β = variable, dimensionless; also $(1-M^2)^{1/2}$, dimensionless
γ = ratio of specific heats, dimensionless
Δ = small change, dimensionless
ϵ = dimensionless small quantity, $0<\epsilon<<1$
η = coordinate ($\bar{y}$-direction), cm
λ = wavelength, cm
υ = inverse radius of curvature, cm^{-1}
ξ = coordinate ($\bar{x}$-direction), cm; also transonic similarity parameter, dimensionless
ρ = density, kg mass/m^3
σ = standard deviation of Gaussian beam, cm
τ = thickness ratio, dimensionless
Ω = angular velocity, rad/sec

Superscripts

$()'$ = dimensionless quantity
$\bar{()}$ = normalized quantity; also average value of a quantity
$(\tilde{})$ = perturbation quantity

Subscripts

i = x-direction or streamline index – first subscript ($i=1$ denotes freestream conditions)
j = y-direction or normal index – second subscript ($j=1$ denotes centerline conditions)
L = linear value
0 = total or stagnation condition; also, peak value of an intensity distribution
w = wall or surface value
∞ = freestream condition

Introduction

THE optical quality of a propagating laser beam is degraded when there are density gradients in the medium. A laser beam propagating through an absorbing medium creates local changes in the density which affect the index of refraction of the medium. Therefore, the density gradients will refract the light into regions of higher index of refraction (higher density) causing defocusing of the beam. This process, which is known as thermal blooming, has been studied by many authors[1-3] to determine the effect on a laser beam propagating through the atmosphere.

When a laser beam is slued, a complicated coupled process of thermal expansion and fluid flow (relative winds) takes place. Depending on the rate of sluing, the beam will experience subsonic, transonic, and supersonic winds at various radial distances from the laser source. The subsonic and supersonic thermal blooming problems have been solved.[4-8]

Received April 30, 1976. This research was supported by Air Force Weapons Laboratory, Kirtland AFB, N. Mex. Contract monitors were Major Keith Gilbert and Dr. Barry Hogge, Laser Divison.

Index categories: Subsonic and Transonic Flows; Radiatively Coupled Flows and Heat Transfer; Lasers.

*LCDR, Ph.D., USN, Graduate Student, Department of Aeronautics.

‡Distinguished Professor and Chairman, Department of Mechanical Engineering. Fellow AIAA.

in which mixed subsonic and supersonic flow exists, and, in particular, the case when the Mach number is precisely unity; that is, at a radial position given by Eq. (1).

A computer program (BLOOM) has been developed and experimentally verified[9] for beam interaction with supersonic flows internal to a Gas Dynamic Laser.

A solution for the transonic regime, and, in particular, the case when the freestream Mach number is precisely unity, has been of considerable interest because the addition of heat can lead to extremely strong density gradients. As with the theoretical investigation of transonic flows over airfoils and wedges, the linear small perturbation flow equations valid for subsonic flow (elliptic equations) and supersonic flow (hyperbolic equations) are no longer valid in the transonic regime.

Many authors[10-15] have studied various methods of solving the transonic flow equations without heat addition. The assumptions based on known transonic behavior about airfoils and wedges are used to simplify the governing equations and, further, to obtain approximate numerical solutions. Often, the assumptions greatly restrict the types of transonic flows that can be solved. For example, in the parabolic method,[16] the transonic flow equation is transformed into a parabolic differential equation. Since the solutions to parabolic differential equations are well established in the literature, this method may be useful when the acceleration or deceleration is constant in the region of interest (i.e., across the cord of many airfoils); however, this method is not valid in the region of the stagnation point or where the flow acceleration changes sign.

With heat addition, the basic flow equations for transonic flow become more complicated. Zierep[17] has solved the case when the Mach number is precisely unity; but, in solving the equation, he has reduced the problem to that of one dimension. Others[18,19] have solved the nonsteady transonic equation with heat addition; however, the results are valid only for a short time after beam turn on (i.e., no steady-state solution). Even for the short time solutions, extrapolation techniques between the property values at the critical points on the subsonic side and the supersonic side are employed to obtain the values across the transonic regime. Experimental investigations are being conducted[20] to determine the influence of transonic sluing on thermal blooming. These experiments indicate that a steady two-dimensional solution is possible. Further experimentation will provide better guidelines for a theoretical analysis of the problem.

In this paper, transonic thermal blooming in steady two-dimensional invisid flow is formulated and solved for a Gaussian heat release distribution. In particular, it examines the problem when the freestream Mach number is preceisely unity. This is accomplished by using a method developed by Broadbent[21-25] in which the streamlines throughout the flow are adjusted so that the heat addition necessary to achieve these streamlines equals the required heat distribution and boundary conditions. The method is exact since specifying the streamlines reduces the nonlinear coupled momentum equations in natural (streamline) coordinates to simple algebraic linear difference equations that can be "marched" through the entire flowfield. Boundary conditions are the freestream properties upstream of the heat release region and the flow properties along a bounding streamtube sufficiently removed from the heat release region that the flow is considered isentropic. The boundary conditions on the bounding streamtube are calculated by methods similar to those employed in determining the velocity and pressure distributions over airfoils of known shape. Since stagnation points do not exist on the bounding streamtube flow, a modification to the method by Sprieter and Alksne[10] for airfoils and wedges was developed.

II. Theory

A laser beam that is slued through the atmosphere at a constant rate of Ω rad/sec will experience regions of subsonic, transonic, and supersonic flow in planes perpendicular to its axis at various radial positions along the beam; Fig. 1. The region to be investigated in this paper is the transonic region

$$r^* = \sqrt{\gamma RT}/\Omega \tag{1}$$

For this analysis, the laser beam is initially of a given axisymmetric Gaussian intensity sluing into an isotropic, quiescent medium of constant density ρ(kgm m^{-3}). Viscosity and thermal conductivity are neglected. The heating effect of the laser beam on the medium is approximated by a molecular relaxation process which is rapid enough that the absorbed energy is instantaneously transformed into heat. The energy distribution is of the form given in Eq. (2)

$$Q = I\alpha = I_0\alpha \exp\left(-\frac{(x^2+y^2)}{2\sigma^2}\right) \tag{2}$$

where Q (Wcm^{-3}) is the time rate of heat absorbed per volume; I_0 (Wm^{-2}) is the beam maximum intensity; α (cm^{-1}) is the absorption coefficient; and the exponential of the Gaussian with standard deviation σ(cm), which is related to the spot size of the beam by $w=\sqrt{2}\sigma$, is centered at the origin of the $x-y$ coordinate system transverse to the beam axis at r^*.

The theory employed for this investigation separates the steady transonic flow with heat addition into two flow regimes; Fig. 2. The solution in the internal heat addition region is calculated exactly by the Broadbent method,[21] in which the nonlinear equations of motion and the energy equation are solved numerically in natural coordinates. Boundary conditions are obtained from the external, isentropic flow region by the transonic solution over a bounding streamtube to the internal region. The shape of the bounding streamtube can be determined. See subsequent discussion.

Broadbent's method[21] is an inverse solution in which the streamlines, normals, and boundary conditions along at least one streamline and normal are specified and the resulting flowfield calculated. The governing equations in natural coor-

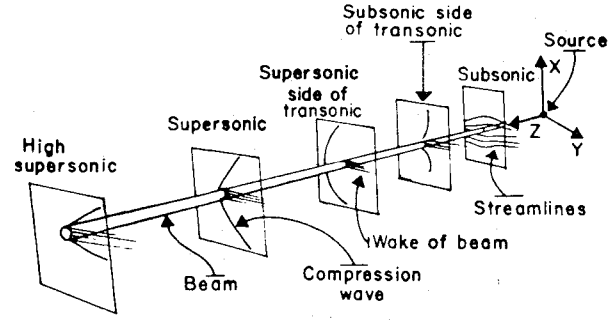

Fig. 1 Flow regimes along a sluing laser beam.

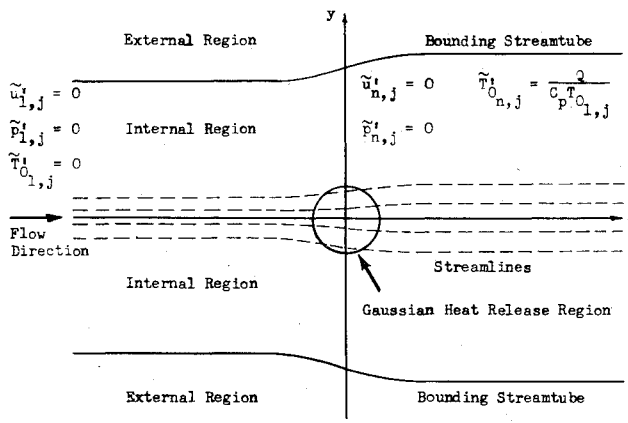

Fig. 2 Transonic flow geometry with heat addition.

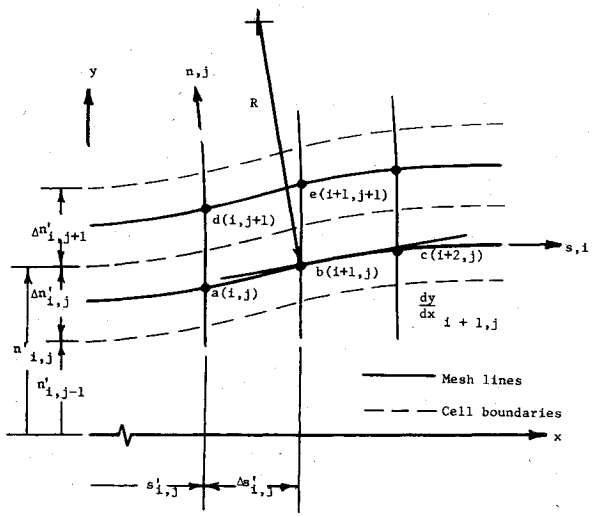

Fig. 3 Natural coordinate system with flow mesh.

dinate for flow with heat addition, but without viscosity, heat conduction or body forces[26] are

$$(\partial/\partial s)(\rho u \Delta n) = 0 \tag{3}$$

$$\rho u(\partial u/\partial s) + (\partial p/\partial s) = 0 \tag{4}$$

$$\rho(u^2/R) + (\partial p/\partial n) = 0 \tag{5}$$

$$\rho u(\partial/\partial s)[h + (u^2/2)] = I\alpha \tag{6}$$

A mesh is constructed over the flowfield using streamlines and normals which are chosen in advance, as in Fig. 3. The cells specify the streamtube boundaries; and the mesh lines, the streamline slope ($dy/dx \cong dn/ds$) and curvature R throughout the flowfield. With the mesh specified, Eqs. (3-6) are nondimensionalized using uniform freestream flow properties ($u_{1,j}$, $p_{1,j}$, $\rho_{1,j}$, and $T_{1,j}$), a constant uniform streamtube width upstream of the perturbations ($\Delta n'_{1,j}$) and constant C_P.

$$\rho'_{i,j} u'_{i,j} \Delta n'_{i,j} = 1 \tag{7}$$

$$\tilde{u}'_{i+1,j+1} - \tilde{u}'_{i,j+1} = \frac{\overline{\Delta n'_{(i,i+1),j}}}{\gamma M_\infty^2} \quad (\tilde{p}'_{i+1,j+1} - \tilde{p}'_{i,j+1}) \tag{8a}$$

$$\tilde{p}'_{i+1,j+1} - \tilde{p}'_{i+1,j} = -\tfrac{1}{2}\gamma M_\infty^2 (u'_{i+1,j+1} v'_{i+1,j+1} + u'_{i+1,j} v'_{i+1,j}) \tag{8b}$$

$$p'_{i,j} = \rho'_{i,j} R T'_{i,j} \tag{9}$$

$$\tilde{T}'_{i+1,j+1} - \tilde{T}'_{i,j+1} + \left[\frac{M_\infty^2(\gamma+1)}{2}\right](u'^{\,2}_{i+1,j+1} - u'^{\,2}_{i,j+1})$$

$$= \left[\frac{\overline{(I\alpha \Delta n')}_{(i,i+1),j}}{Q_\infty}\right] \Delta s'_{i,j+1} = Q'_{i,j+1} \tag{10a}$$

$$Q_\infty = \left[\frac{\rho_\infty u_\infty C_p T_\infty [1 + [(\gamma-1)/2]M_\infty^2]}{\Delta n_{1,j}}\right]$$

$$= \frac{p_\infty u_\infty (1 + [(\gamma-1)/2]M_\infty^2)\gamma}{\Delta n_{1,j}(\gamma-1)} \tag{10b}$$

$Q'_{i,j+1}$ is a dimensionless heating term; and $v'_{i,j}$ is a dimensionless inverse radius of curvature ($\Delta n_{i,j}/R$).

Equations (8a) and (8b) represent two nonlinear equations since $\tilde{u}, \tilde{p}, \Delta n'$ and v' are dependent variables. However, specifying the streamlines of the flow, these equations become linear equations solvable for $\tilde{u}_{i+1,j+1}$ and $\tilde{p}_{i+1,j+1}$ at point e in terms of $\tilde{u}_{i+1,j}, \tilde{p}_{i+1,j}$ at point d and $\tilde{u}_{i,j+1}$, $\tilde{p}_{i,j+1}$ at point b; Fig. 3. The remaining flow properties $\tilde{\rho}_{i+1,j+1}$ and $\tilde{T}_{i+1,j+1}$ can be calculated from the continuity equation, Eq. (7), and equation of state, Eq. (9). However, the new properties at the point $e(i+1,j+1)$ may not satisfy the energy equation, Eq. (10). If it is not satisfied, an iteration process is performed by varying the streamline distribution and by recalculating the properties until coincidence exists throughout the entire flowfield. Hence, the solution of the problem is reduced to finding the streamline distribution that satisfies Eqs. (7-10) and the boundary conditions determined from the external region.

Insight into the behavior of the streamlines at the sonic speed was obtained from the solution of the linearized small perturbation equation with heat addition.[7,8] A computer program (BLOOM) was devised which gave solutions for a flow very slightly below the sonic speed ($M_\infty = 0.999$) and very slightly above the sonic speed ($M_\infty = 1.001$). Computations of the nonlinear term in the transonic small perturbation equation[26] from the linear results indicate that the linear equations are valid to $M_\infty = 0.9999$ subsonically and $M_\infty = 1.0001$ supersonically. From the linear solutions, a trend of the streamline shape was obtained in the near sonic regime, even if not at sonic conditions. Nature usually exhibits a strong propensity to accomplish changes in a rather smooth fashion (even a shock wave is a smooth change in conditions if viewed microscopically enough); thus, a knowledge of flow conditions in the near sonic range gives a good clue to the sonic flow behavior.

The streamlines are found to spread as the beam is passed in a similar manner immediately below and immediately above the sonic speed. Figure 2 is a sketch of the general streamline shape. It was expected, therefore, that the streamline behavior at the sonic speed would not vary radically from this pattern. Based on the streamline distribution in Fig. 2, the following relationship between area change (streamtube width variation) and change in total temperature (heat input) was chosen,

$$\frac{dA}{A} = \frac{dn}{n} = \frac{(\gamma+1)(1+\beta)}{2}\frac{dT_0}{T_0} \tag{11}$$

where T_0 is the local total temperature of the flow and β is a variable. One-dimensional influence coefficients with area change and heat addition,[27] Eq. (12), were used to determine the required β at precisely Mach 1.0

$$\frac{dM^2}{dx} = \frac{G(x)}{(1-M^2)} \tag{12}$$

where

$$G(x) = M^2(1 + \tfrac{1}{2}(\gamma-1)M^2)\left(-2\frac{d\ln(n)}{dx} + (1+\gamma M^2)\frac{d\ln(T_0)}{dx}\right)$$

In order for Eq. (12) to remain finite and to be defined at Mach 1.0, $G(x)$ must tend to zero in the limit as the Mach number approaches unity. If Eq. (11) is substituted into Eq. (12) and the limit taken, it is found that β must be zero at precisely Mach 1.0. Hence, the streamtube area change is related to the heat input by Eq. (13).

$$\frac{dn'_{i,j}}{n'_{i,j}} = \frac{(\gamma+1)}{2}\frac{dT'_{0i,j}}{T'_{0\,1,j}} \tag{13}$$

where the difference between $n'_{i,j}$ and $n'_{1,j}$, and $T'_{0i,j}$ and $T'_{01,j}$ is of the order of 10^{-6} and, hence, the freestream values can

be used in the denominator. Using this approximation for the streamtubes, an explicit formulation of the streamtube shape, slope, and radius of curvature at any position $s'_{i,j}$ along a streamtube, was obtained.

Consequently, the proportionality between the streamtube shape and heat release distribution gives not only an explicit formulation for the streamtubes and, hence, linearization of the nonlinear momentum equations but also simultaneous agreement between those properties calculated with the momentum equations and the energy equation. The problem,in the case of precisely $M_\infty = 1.0$ flow, becomes one of determining the correct boundary conditions.

The boundary conditions that are used are those corresponding to freestream conditions ($\tilde{u}'_{I,j} = \tilde{p}'_{I,j} = \tilde{\rho}'_{I,j} = \tilde{T}'_{I,j} = 0$), which are far enough upstream that the properites are not affected by the perturbation caused by the heat release region, and the pressure (p'_{i,j^*}) and/or velocity (u'_{i,j^*}) on the j^*th streamtube which is considered far enough removed from the heat release region that the flow can be considered isentropic. Since the streamtube shape is known throughout the heat addition region, the streamtube shape and displacement where $j = j^*$ can be calculated. The bounding streamtube can be considered as a solid wall similar to the surface of a wedge with a cusp extending forward to the freestream conditions upstream at infinity; Fig. 2. By hypothesis, this flow is isentropic and can be treated by methods similar to those used in analyzing transonic airfoil and wedge flows. In particular, an approximate solution is obtained through an iteration process on the integral equation derived from Green's functions for small disturbance transonic flow similar to Sprieter and Alksne[10,11] for thin airfoils and wedges. The derivation was modified for the streamtube configuation because no stagnation points exist. The absence of stagnation points in the case of the flow around the bounding streamtube enhances the accuracy of the approximate numerical techniques because the stagnation point represents a singularity in the problem and places added constraints on the method and accuracy of the solution in the region of the stagnation point. In the modified Sprieter-Alksne method, the quadratic, nonlinear nature of the governing equations is retained which precludes shock-free supercritical flows in the transonic regime. Shock waves are an essential aspect of the flow.

The integral equation for transonic flow is derived by a Green's function analysis of the small perturbation transonic equations without heat addition,[26] resulting in Eq. (14).

$$\bar{u}_w(\bar{x},o) = \bar{u}_{Lw}(\bar{x},0) + \frac{u_w^{-2}(\bar{x},0)}{2} - I/2 \tag{14}$$

where

$$\bar{u}_w(\bar{x},0) = \frac{M_\infty^2(\gamma+1)\bar{u}'(x,0)}{\beta^2} = \frac{M^2 - M_\infty^2}{\beta^2} \tag{15}$$

$$\bar{u}_{Lw}(\bar{x},0) = (1/\pi)\int_{-\infty}^{\infty} \frac{d\bar{Z}}{d\bar{\xi}} \frac{d\bar{\xi}}{(\bar{x}-\bar{\xi})} \tag{16}$$

$$I = \int_{-\infty}^{\infty} \frac{u_w^2(\bar{x},0)}{b} E\left(\frac{\bar{\xi}-\bar{x}}{b}\right) d\bar{\xi};$$

$$E\left(\frac{\bar{\xi}-\bar{x}}{b}\right) = -\frac{b}{2\pi}\int_{-\infty}^{\infty} \frac{\partial^2}{\partial\bar{\xi}^2}\left[\ln\frac{r_1}{r_2}\right] d\bar{\eta} \tag{17}$$

and the normalized variables are defined in Ref. 10. Equation (14) is a function of only $\bar{x}$, the normalized coordinate along the wall surface. The normalized amplitude of the wall slope $\bar{\tau}$, is given by:

$$\frac{d\bar{Z}}{d\bar{x}} = \bar{\tau}\exp - \frac{\bar{x}^2}{2\bar{\sigma}^2} \tag{18a}$$

where

$$\bar{\tau} = \frac{M_\infty^2(\gamma+1)\tau}{\beta^3} = \frac{M_\infty^2(\gamma^2-1)I_0\alpha\sqrt{2\pi}\sigma}{\beta^3 p_\infty u_\infty \gamma} \tag{18b}$$

The iteration technique is performed for various freestream subsonic Mach numbers starting at the initial supercritical flow and proceeding toward the Mach 1.0 flow. Each solution obtained by the iteration technique gives a unique $\bar{\tau}$, which determines the freestream Mach number and its corresponding normalized velocity distribution $\bar{u}_w(\bar{x},0)$ along the surface. If $(\bar{u}_w - 1)$vs $\bar{\tau}^{2/3}$ is plotted for each position along the surface, it is found that as the freestream Mach number tends toward unity the slope becomes constant. Constant slope corresponds to the phenomenon of the Mach number freeze[26] wherein the local Mach number is invariant with changes in the freestream Mach number when the latter is near unity or, more precisely

$$\left.\frac{dM}{dM_\infty}\right]_{M_\infty = 1} = 0 \tag{19}$$

The corresponding approximate relation yielded by the small-disturbance transonic theory[28-30] is given by:

$$\left.\frac{d\xi}{d\xi_\infty}\right]_{\xi_\infty = 0} = 0 \tag{20}$$

where,

$$\xi = -\frac{(1-M^2)}{(M_\infty^2(\gamma+1)\tau)^{2/3}} = \frac{(\bar{u}-1)}{\bar{\tau}^{2/3}} \tag{21}$$

The freeze of Mach number extends over a finite range near Mach 1.0 where ξ is constant. Hence ξ, the slope of $(\bar{u}-1)$ vs $\bar{\tau}$ at each location $\bar{x}$, is constant near the sonic condition, and the local Mach number at each position can be calculated by Eq. (21). With the local Mach number distribution known, the velocity perturbation can be calculated from Eq. (15), and the other flow properties can be determined from isentropic flow relations.[27]

The Mach 1.0 flow is completely specified. Boundary conditions are known upstream of the heat release region and on a bounding streamtube. Calculation of the entire flowfield is readily calculated from the simple algebraic equations obtained by Broadbent's method where the streamtube configuration is known precisely at Mach 1.0.

III. Numerical Results

The computed flow properties are for the Mach 1.0 thermal blooming problem with the characteristics listed in Table 1.

The first step in the procedure is to determine the boundary conditions for the heat release region. Far upstream of the heat release region, all the dimensionless perturbation quantities are zero. The other boundary conditions are calculated

Table 1 Flow characteristics

Gaussian beam	
Peak intensity (I_0)	3.333×10^7 W/m^2
Standard deviation (σ)	5 cm.
Atmospheric absorption (α)	8.0×10^{-7}cm^{-1}
Atmospheric freestream conditions	
Temperature (T_∞)	288.0 °K
Pressure (p_∞)	1.013×10^5N/m^2
Density (ρ_∞)	1.2246 kgm/m^3
Velocity ($u_\infty = a^*$)	340.0 m/sec
Streamtube width ($\Delta n_{I,j} = \Delta n_\infty$)	1 cm
Streamline cell length ($\Delta s_{i,1}$)	1 cm
Ratio of specific heats (γ)	1.4
Specific heat at constant pressure (C_p)	1005.0 J/kgm °K

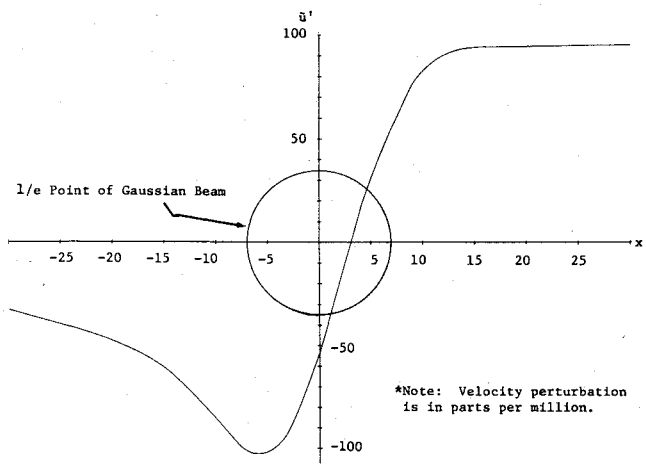

Fig. 4 Velocity perturbations on bounding streamline at $M_\infty = 1.00$.

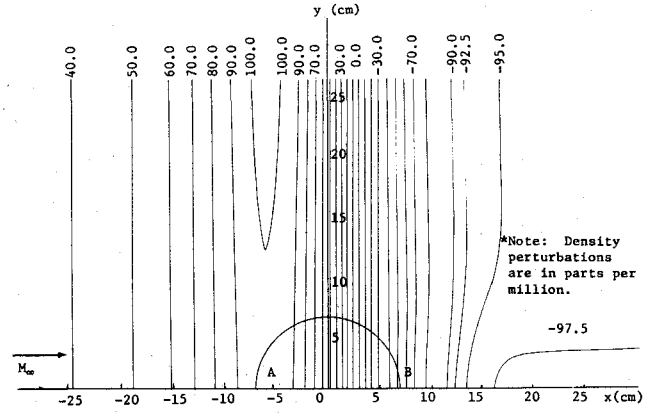

Fig. 5 Density perturbations for $M_\infty = 1.00$ and a Gaussian beam.

by Sprieter's method[10] for the bounding streamtube, the shape of which depends upon the heat release distribution and is known.

Using Sprieter's numerical iteration procedure on the transonic flow integral equation, Eq. (14), the normalized velocity distribution along the bounding streamtube was obtained for several freestream Mach numbers between the initial supercritical flow and Mach 1.0. Next, using these solutions, a $(\bar{u}-1)$ vs $\bar{\tau}^{2/3}$ curve was plotted for several positions along the streamtube. The results indicate that the slope (ξ) is constant for each position and, hence, the Mach number can be considered frozen.

From the values of $\xi(\bar{x})$, the local Mach number variation at a freestream Mach number of unity was calculated from Eq. (21), since ξ is known and constant for the known physical streamtube shape.

$$\tau = \frac{t}{\sqrt{2\pi\sigma}} = 1.386 \times 10^{-6} \qquad (22)$$

where

$$t = \frac{(\gamma-1) I_0 \alpha \pi \sigma^2}{\gamma p_\infty u_\infty} = 1.737 \times 10^{-5}\,\text{cm}.$$

is the maximum growth of the bounding streamtube.

Once the local Mach number was determined, the velocity perturbation along the bounding streamtube was calculated from Eq. (15) and is plotted in Fig. 4. The remaining flow properties were calculated by the isentropic flow relations.[27]

It has been shown that the area change of the streamtubes in the heat addition region is directly proportional to the change in total temperature; that is, $\beta = 0$ in Eq. (11). The energy

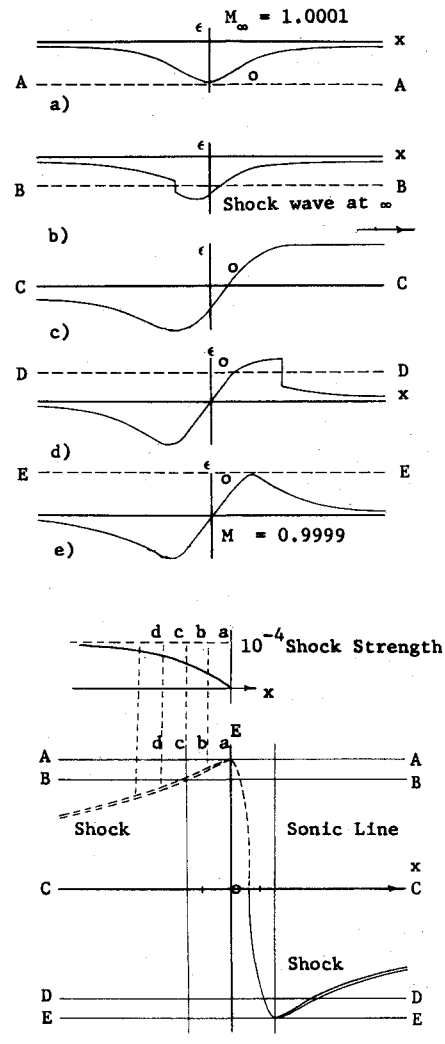

Fig. 6 Mach number distribution in the plane of symmetry through laser beam for transonic flow: a) supersonic flow; b) supersonic supercritial flow; c) sonic flow; d) subsonic supercritial flow; e) subsonic flow; f) Mach number $(M = 1 + \epsilon)$ vs position along beam centerline in the transonic regime (dashed line represents hypothesized supersonic behavior).

equation is automatically satisfied by this selection for the area variation. Since the heat release distribution is known, all of the streamtubes and hence the radii of curvature at every point throughout the region are known.

With the curvature known, the calculation of the flow properties in the heat region is reduced to the solution of two simple linear algebraic equations, Eqs. (8a) and (8b), which are the momentum equations in natural coordinates. The results of this "marching" technique are shown in Fig. 5 where the density perturbations in the upper half of the symmetric laser beam are presented. This method is numerically straightforward and has the distinct advantage that it can be readily solved on a desk top computer (i.e., HP9830, etc.). The results presented in Fig. 4 at Mach 1.0 are consistent with a continuous transition through the transonic regime. Although the solutions calculated are for subsonic M_∞ and for precisely Mach 1.0, it can be logically hypothesized that the flow behavior through the transonic regime is as shown graphically in Fig. 6. The flow for supersonic M_∞ was not calculated. The linear supersonic and subsonic solutions and the high subsonic solutions are in excellent agreement with this hypothesis. Therefore, there is a steady, two-dimensional solution for the transonic thermal blooming problem which is finite and does not result in "catastrophic" defocusing of the

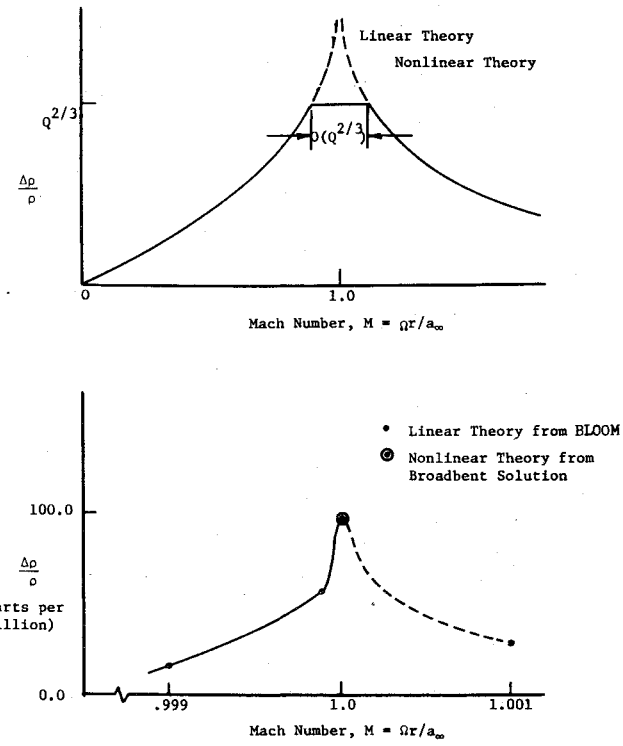

Fig. 7 Schematic representation of the steady-state density perturbations for a sluing two-dimensional laser beam: a) results of Ellinwood and Mirels; b) results of linear subsonic and supersonic solutions from BLOOM and nonlinear solution at $M_\infty = 1.00$.

laser beam. Details of the analysis and the calculations can be found in Carey's dissertation.[31]

IV. Conclusions

It has been demonstrated that there is a two-dimensional, steady-state solution to the transonic thermal blooming problem for a sluing laser beam with a freestream Mach number of precisely unity. According to the linearized solutions for thermal blooming, the density perturbations become infinite as a Mach number of unity is approached. Due to nonlinear effects the trend to infinity is terminated, and the finite value of perturbation quantities has been established.

In obtaining the solution, it was found that at precisely Mach 1.0 the streamtube area variation through the heat release region is directly proportional to the change in total temperature in that region. With the streamtube shapes known, an exact solution for the flow field can be obtained by Broadbent's method[21] using the boundary values for Mach 1.0 isentropic flow far from the heat release region. There are no restrictions on the existence of shock waves nor on the symmetry or asymmetry of the heat release distribution, provided the bounding streamtube in the isentropic region and the boundary conditions on it can be calculated.

Furthermore, in obtaining the solution at precisely Mach 1.0, it was found that shock waves exist throughout the transonic regime; Fig. 6. As the sonic condition is approached from subsonic speeds, a shock wave forms at the downstream $1/e$ (one spot size) point of the Gaussian heat release distribution and rapidly moves downstream to infinity. If the sonic speed is approached supersonically, a shock is formed at the beam center. To be consistent with the results in the subsonic portion of the transonic regime, it has been hypothesized that the shock moves rapidly upstream to infinity. Finally, the analysis in the Appendix indicates that there is a minimum laser sluing rate that must be maintained to preclude significant phase distortion in the beam at Mach 1.0. A fast slue rate decreases the extent of the transonic region.

The results of the Mach 1.0 thermal blooming problem for a Gaussian intensity distribution are in excellent agreement with the approximate results obtained by Ellinwood and Mirels.[19] Figure 7 shows these results where the maximum density perturbation was calculated to be of the order of $Q^{2/3}$. Q is defined as:

$$Q = \frac{(\gamma - 1) I_0 \alpha r}{\gamma p a} \tag{23}$$

where r is the radius (spot size) of a circular beam of uniform heating intensity ($I_0\alpha$). This approximation, when applied to the Gaussian beam of the previous section, gives a maximum density perturbation of the order of 10^{-4} which is consistent with that obtained in this paper and shown in Fig. 7. Although the density perturbations are very small (i.e., measured in parts per million), significant optical defocusing of the laser beam could result as is demonstrated in the Appendix. With an increase in the beam area due to defocusing, a significant decrease in the beam intensity I (W/m^2) will occur.

Two other methods that show promise in solving the transonic thermal blooming problem are the finite difference method developed by Murman and Cole[12] for isentropic transonic flow, which can be extended to include heat addition, and the "finite-element method" of solving partial differential equations;[32] the finite-element method is a powerful techique for solving a wide range of engineering problems.

Appendix: Derivation of the Sluing Rates Necessary to Preclude Significant Phase Distortions in a Laser Beam at Mach 1.0

When the phase difference between two points in a laser beam is greater than a quarter of a wavelength, the deviation of the beam from its original direction may be sufficient to cause considerable distortion. The range of laser sluing rates necessary to prevent such phase distortions and, hence, to preclude defocusing of the beam at Mach 1.0 is derived.

Consider a laser beam that is slued as shown in Fig. 1. The Mach number of the air relative to the beam varies along the beam as:

$$M = U/a = \Omega r/a \tag{A1}$$

All Mach number regimes occur along the beam. If L represents the radial distance between two stations on the beam where the Mach numbers are M_1 and M_2, it can be determined from Eq. (A1) that L is equal to:

$$L = \frac{(M_2 - M_1)a}{\Omega} \tag{A2}$$

The number of waves N of laser radiation in the region of length L is given by:

$$N = \frac{L}{\lambda} = \frac{n\nu L}{c} \tag{A3}$$

where λ is the wavelength of the laser beam and is equal to $n\nu/c$, ν (rad sec^{-1}) is the laser frequency equal to approximately 2×10^{13} Hz for a CO_2 laser, and c (m sec^{-1}) is the speed of light. Therefore, the change in the number of waves in the beam length L, due to a change in the index of refraction, is obtained by differentiating Eq. (A3).

$$dN = \frac{\nu L dn}{c} \tag{A4}$$

The change in the refractive index is related to the density perturbations in the beam, a known quantity, through the

Gladstone-Dale Law,[32] a simplified version of the Lorentz-Lorenz Law for gases with $n \cong 1$.

$$n = 1 + k\rho \tag{A5}$$

where k is the Gladstone-Dale constant which is approximately equal to 2.25×10^{-4} m^3/kgm for air with wavelengths beyond the near infrared. Differentiating Eq. (A5) and substituting it and Eq. (A2) into Eq. (A4), the desired expression for the change in the number of waves is obtained as

$$dN = \left(\frac{k(M_2 - M_1) a v \rho_\infty}{\Omega c} \right) \frac{d\rho}{\rho_\infty} \tag{A6}$$

It is of interest to determine the range of sluing rates for which the change in the number of waves is less than a quarter of a wavelength at Mach 1.0 from Eq. (A7):

$$\Omega > \frac{4k(M_2 - M_1) a v \rho_\infty}{c} (\tilde{\rho}'_{\text{Max}} - \tilde{\rho}'_{\text{Min}}) \tag{A7}$$

where $\tilde{\rho}'_{\text{Max}}$ is the maximum positive density perturbation and $\tilde{\rho}'_{\text{Min}}$ is the minimum (maximum negative) density perturbation in the flow field at Mach 1.0, points A and B in Fig. 5, respectively. As an example, using $M_2 = 1.001$, $M_1 = 0.999$, the flow properties in Table 1, and the maximum difference in the density perturbations at Mach 1.0 from Fig. 5 of 1.5×10^{-4}, the sluing rate must be greater than 7.5×10^{-3} rad/sec.

References

[1] Lehnigk, S.H. and Steverding, B., "High Intensity Light Propagation and Induced Natural Laminar Flow," U.S. Army Missile Res., Devel., and Eng, Lab., U.S. Army Missile Command, Redstone Arsenal, Ala.

[2] Rosenstock, H.B. and Tucker, J.W., "An Upper Limit on the Thermal Defocusing of a Light Beam," NRL Memorandum Report 2109, April 1970.

[3] Tucker, J.W. and DeWitt, R.N., "Atmospheric Propagation with Thermal Blooming," NRL Report 7038, Dec. 1969.

[4] Fuhs, A.E., "Density Inhomogeneity in a Laser Cavity due to Heat Release," *AIAA Journal*, Vol. 11, March 1973, pp. 374-375.

[5] Biblarz, O. and Fuhs, A.E., "Laser Cavity Density Changes with Kinetics of Energy Release," *AIAA Journal*, Vol. 12, Aug. 1974, pp. 1083-1089.

[6] Biblarz, O. and Fuhs, A.E., "Laser Internal Aerodynamics and Beam Quality," *Developments in Laser Technology—II*, Vol. 41, Society of Photo Optical Instrumentation Engineers, 1973.

[7] Fuhs, A.E., Biblarz, O., and Carey, E.F., "Thermal Blooming in Supersonic Slewing," *Bulletin of American Physical Society*, Vol. 18, Nov. 1973, p. 1485. Abstract only.

[8] Burden, H.W., Biblarz, O., and Fuhs, A.E., "Thermal Blooming in Subsonic Slewing," *Bulletin of American Physical Society*, Vol. 18, Nov. 1973, p. 1490. Abstract only.

[9] Fuhs, A.E., Biblarz, O., Cawthra, J.K., and Campbell, J.L. "Experimental Verification of Density Inhomogeneity due to Lasing in a Gas-Dynamic Laser," *Applied Physics Letters*, Vol. 24, Feb. 1974, pp. 132-134.

[10] Sprieter, J.R. and Alksne, A.Y., "Theoretical Prediction of Pressure Distribution on Nonlifting Airfoils at High Subsonic Speeds," NACA, TN 3096, Mar. 1954.

[11] Sprieter, J.R. and Alksne, A.Y., "Thin Airfoil Theory Based on Approximate Solution of the Transonic Flow Equation," NACA Report 1359, 1958.

[12] Murman, E.M., and Cole, J.D., "Calculation of Plane Steady Transonic Flow," *AIAA Jorunal*, Vol. 9, Jan. 1971, pp. 114-121.

[13] Hosokawa, I., "Transonic Flow Past a Wavy Wall," *Journal of the Physical Society of Japan*, Vol. 15 Nov. 1960, pp. 2080-2086.

[14] Guderley, K.G., *The Theory of Transonic Flow*, Pergamon Press, 1962.

[15] Guderley, K.G. and Yoshihara, H., "The Flow over a Wedge Profile at Mach Number 1," *Journal of Aeronautical Sciences*, Vol. 17, Nov. 1950, pp. 723-735.

[16] Oswatitsch, K. and Keune, F., "The Flow Around Bodies of Revolution at Mach Number 1," *Proceedings of the Conference on High Speed Aeronautics*, Polytechnic Institute of Brooklyn, 1955.

[17] Zierep, J. "Schallnahe Stromungen mit Warnezufuhr," *Acta Mechanica*, Vol. 8, 1969, pp. 126-132; translated as Royal Establishment Library Translation 1452, Feb. 1970 with English title, "Transonic Flow with Heat Input."

[18] Munn, M.W., "Laser Heat Induced Density Changes is Gases: Dependence upon Time and Transverse Flow Velocity, I." Lockheed Missiles and Space Co., Report D356026, Nov. 1973 revised Jan. 1974.

[19] Ellinwood, J.W. and Mirels, H., "Density Perturbations in Transonic Sluing Laser Beams," Space and Missile Systems Organization, U.S. Air Force, Technical Report 75-98, Mar. 1975.

[20] Brown, R.T., Berger, P.J., Gebhardt, F.G., and Smith, D.C., "Influence of Dead Zones and Transonic Slewing on Thermal Blooming," United Aircraft Research Labs. Mid-term Tech. Rept. Nov. 1973.

[21] Broadbent, E.G., "An Exact Numerical Method of Calculating Inviscid Heated Flows in Two-Dimensions with an Example of Duct Flow," *Ingenieur-Archiv*, Vol. 40, 1971, pp. 14-28.

[22] Broadbent, E.G., "An Extended Numerical Method of Calculating Two-Dimensional or Axisymmetric Heated Flows Allowing for Dissipation," *Ingenieur-Archiv*, Vol. 40, 1971, pp. 81-95.

[23] Broadbent, E.G., "Axisymmetric Flow with Heat Addition to Simulate Base-burning," *Zeitschrift fur Flugwissenschaften*, Vol. 21, Jan. 1973, pp. 1-15.

[24] Broadbent, E.G., "Flowfield Calculations for Some Supersonic Sections with Ducted Heat Addition," *Ingenieur-Archiv*, Vol. 42, 1973, pp. 89-103.

[25] Broadbent, E.G., "Some Shockless Axisymmetric Flows with Heat Addition," *Zeitschrift fur Flugwissenschaften*, Vol. 21, March 1973, pp. 91-101.

[26] Liepmann, H.W. and Roshko, A., *Elements of Gas Dynamics*, John Wiley and Sons, 1957.

[27] Shapiro, A.H., *Compressible Fluid Flow*, Ronald Press Co., New York, Vol. I., 1953, pp. 83-84, 231.

[28] Vincenti, W.G. and Wagoner, C.B., "Transonic Flow Past a Wedge Profile with Detached Bow Wave-General Analytical Method and Final Calculated Results," NACA, TN2339, 1951.

[29] Liepmann, H.W. and Bryson, A.E., Jr., "Transonic Flow Past Wedge Sections," *Journal of Aeronautical Sciences*, Vol. 17, Dec. 1950, pp. 745-755.

[30] Bryson, A.E., Jr., "An Experimental Investigation of Transonic Flow Past Two-Dimensional Wedge and Circular-Arc Sections Using a Mach-Zehnder Interferometer," NACA TN 2560, 1951.

[31] Carey, E.F., "Transonic Thermal Blooming," Naval Postgraduate School, Ph.D. Dissertation, March 1976, available from DDC.

[32] Huebner, K., *Finite Element Method for Engineers*, Wiley Interscience, 1975.